Zeitschrift: Technische Mitteilungen / Schweizerische Post-, Telefon- und Telegrafenbetriebe = Bulletin technique / Entreprise des postes, téléphones et télégraphes suisses = Bollettino tecnico / Azienda delle poste, dei telefoni e dei telegrafi svizzeri

Herausgeber: Schweizerische Post-, Telefon- und Telegrafenbetriebe

Band: 60 (1982)

Heft: 10

Artikel: A survey of today's reflection factor measurement methods in coaxial systems

Autor: Eicher, Bernhard / Staeger, Christian

DOI: https://doi.org/10.5169/seals-876177

A Survey of Today's Reflection Factor Measurement Methods in Coaxial Systems

Bernhard EICHER and Christian STAEGER, Berne

621.317.341.3

The Progress in the field of coaxial reflection factor measurement techniques is characterized by a considerable improvement in accuracy and speed of measurement during the past ten years. Several new methods appeared and a survey of known older methods, a description of new methods and circuits are presented in the following article.

Generally the available measurement methods can be subdivided into three categories:

1 Methods in the frequency domain without error recognition
2 Methods in the frequency domain with error recognition
3 Time domain measuring methods

1 Measuring Circuit in the Frequency Domain without Error Recognition

In *Figure 1* a simple, self explaining set-up is shown using either a bridge, directional coupler or a slotted line. A distinction between errors from different sources is not possible.

The directivity of the measuring device (or the residual reflection in the case of a slotted line) and the test port mismatch are sources of errors, contributing to the unknown value to be determined.

Because every set-up has to be calibrated by a reflection factor of unity, the test port mismatch interacts with this calibration reflection and deteriorates measurement accuracy for reflection factors near unity.

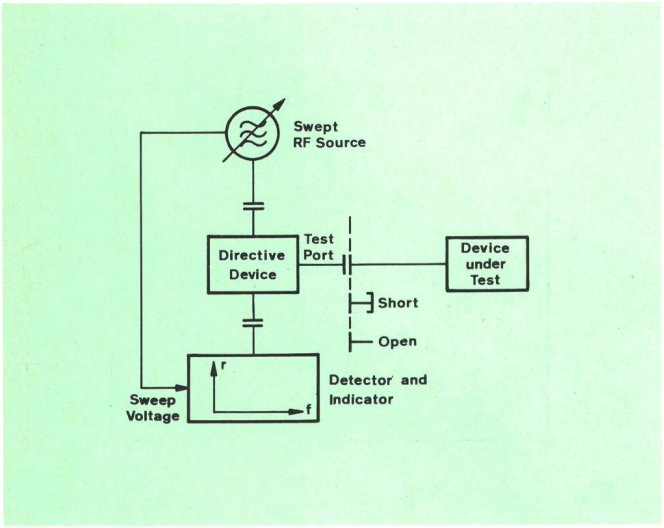

Fig. 1
Simple reflection factor measurement test set-up

Directivity errors affect the calibration far less but begin to dominate measurement inaccurary toward small reflection factors. These two effects are illustrated by the characteristic error plot of *Figure 2.*

Example 1: A bridge set-up with directivity D = 40 dB, testport mismatch $r_{TP} = 0.10$ and unknown reflection $r_x = 0.8$ can be measured as $r_x = 0.73...0.89$

Example 2: A coupler set-up with directivity D = 30 dB, testport mismatch $r_{TP} = 0.10$ and unknown reflection $r_x = 0.1$ can be measured as $r_x = 0.068...0.118$

The normally poor source match of sweep generators can also cause measurement errors, especially when directional couplers are used with their inherent low insertion loss. In such a case it is suggested to use a test set-up according to *Figure 3.*

The additional coupler and leveling circuit reduces the influence of generator source mismatch. The total improvement of source impedance match is limited by the nominal directivity and the main-line reflection factor of the leveling coupler.

When an adaptor is used on the test port to adapt to a different sex or connector type, the measurement accuracy is reduced in two ways. The effective directivity of the measuring device is reduced by the reflection factor of the adaptor and the test port match is degraded as well.

Another source of errors is caused by the spectral impurity of the test signal, especially in devices under test with fast changing frequency characteristics. Recently developed signal sources and sweepers use additional tracking filters to overcome these problems.

A short view of typical specifications of modern directive bridges and directional couplers is given below in *Table I.*

Applications of these test set-ups include scalar (amplitude only) and complex (amplitude and phase) meas-

Table I. Typical specifications of directive bridges and directional couplers

	Bridges	Couplers
Frequency range (broadband)	0.01...18 GHz	0.1...2 GHz 1...18 GHz
Directivity D	40 dB	26...36 dB
Testport r_{TP} mismatch	$r_{TP} = 0.1...0.15$	$r_{TP} = 0.1...0.15$
Loss input-testport	~ 6 dB	0.2...1.0 dB
Coupling	~12 dB	6...20 dB

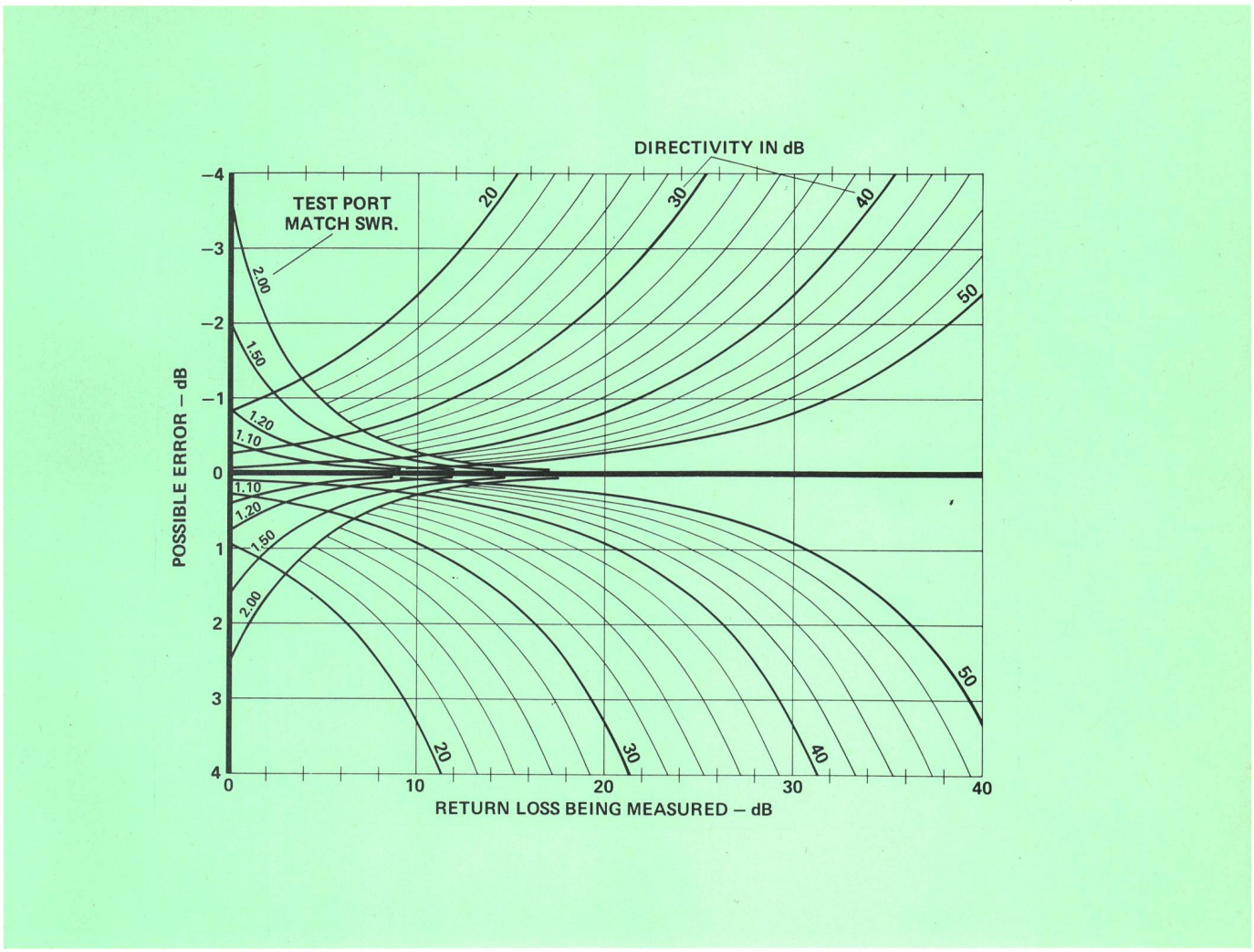

Fig. 2
Error limits for reflection factor measurement

urements on one or two-ports. Note that when two-ports are measured, additional errors appear, caused by non-ideal termination at the output port.

2 Measurement Methods in the Frequency Domain with Error Recognition

State-of-the-art methods allow to reach at least 10 dB better directivity values by applying either computer correction or offset magnifying techniques with respect to the previous described test procedures.

All error recognition systems are referred to reference standards in the form of precise machined coaxial lines, short circuits, open lines and high precision sliding loads.

21 The Automatic Network Analyzer Concept (ANA) [1]

The ANA is in principle a combination of a vector voltmeter, sweep generator and directive device (coupler, bridge), controlled by an appropriate calculator as shown in *Figure 4*.

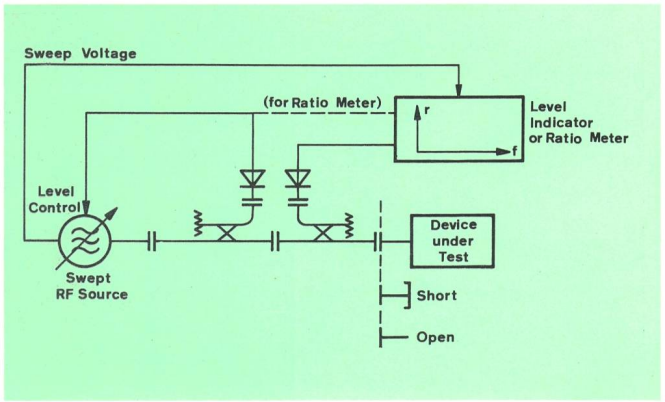

Fig. 3
Set-up with directional couplers with improved source match

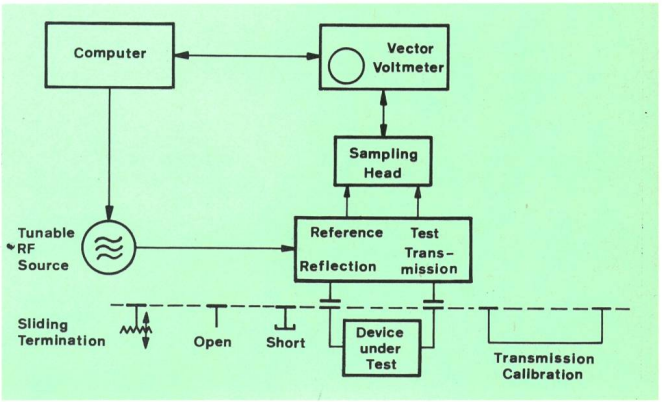

Fig. 4
Automatic network analyzer block diagram

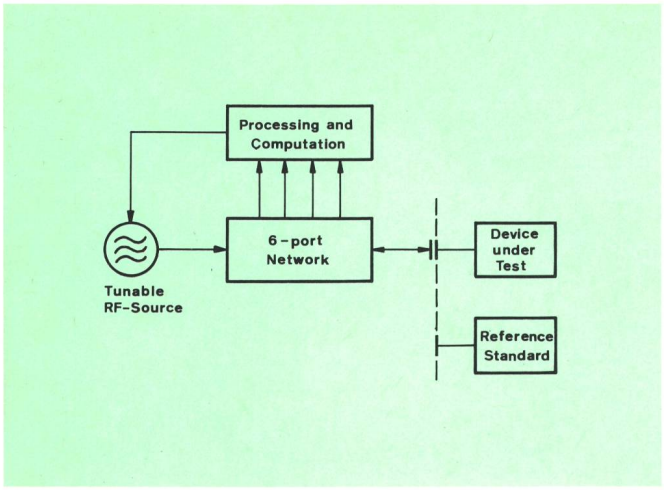

Fig. 5
Six-port measuring configuration

The ANA must first be calibrated within the desired frequency range by means of a short circuit, open line and precision system impedance termination at the test port. Appropriate error correction allows to establish virtual directivities D of 45 to 50 dB and virtual source mismatch of less than $r \leqq 0.1$.

The main advantage of the ANA is precise measurements of phase and magnitude with excellent frequency and amplitude stability.

One of the most precise reflection factor and transmission factor measuring device in the form of a sophisticated ANA has been realized by the National Bureau of Standards (NBS) in the USA.

However, there are some drawbacks:
Slow speed presentation of ANA test data caused by the computer correction routine can be uncomfortable for tuning work on components. Resonance effects on the test item can be lost when they fall between test frequency steps. Real source match conditions can affect measurements on active devices.

An interesting application of the ANA is obtained by applying Fast Fourier Transform (FFT) algorithm to the frequency domain data, which results in a time domain response of the device under test. By applying window functions, discontinuities on an electrically long test object can be discriminated in distance. Another FFT routine transforms the content of the selected data window back to the frequency domain where the complex impedance behaviour can be investigated.

Although these are very powerful methods, there is practically no published data available. A big problem can be the loss of information caused by the discrete nature of the Fourier transforms. Multiple reflections can disturb measurements too.

22 Six-port Measurement System

This recently developed method allows complex transmission and reflection factor measurements by using a six port junction with four amplitude detectors (diodes, power meters) *(Fig. 5)*.

Again reference calibration is established using similar procedure as in the ANA case.

Up to now, the performance of such a system is not well known for the frequency range 0.1...18 GHz, because there is no commercial six-port analyzer available on the market. Besides the original NBS instrument, there are only a few prototypes working with limited success around the world.

Remaining problems are: Calibration procedure depends on measurement problem; limited dynamic range because the power input should be approximately 1 W, harmonics $\leqq 40$ dB below the carrier signal affect measurements, temperature drift of detectors is critical.

23 Magnified Offset Reflection Method [2]

The method is applicable only to display the magnitude of a complex reflection factor. Bridges or directional couplers are used together with precision air lines in order to separate directive device imperfections from the unknown device under test. The method is restricted to reflection factors in the range $r_x = 0.002...0.05$ when the reference port A of the bridge is terminated with a known reflection factor $r_a \cong 0.1$ *(Figure 6)*.

The measurement set-up is first calibrated by terminating port A of Figure 6 with the nominal system impedance and connecting short and open circuits on the test port. Modern instrumentation allows to derive from this measurement the true value of reflection factor unity by averaging.

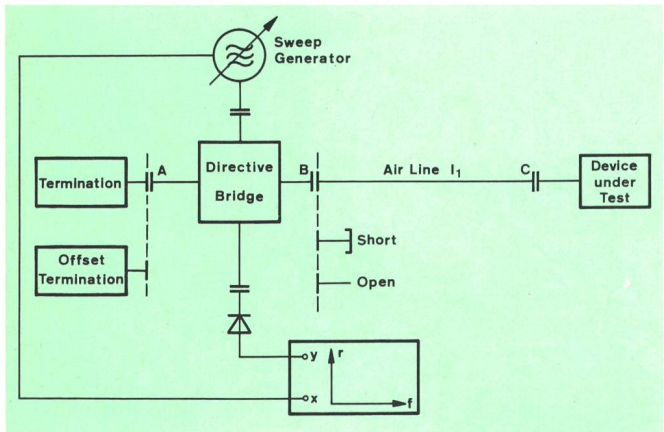

Fig. 6
Magnified offset reflection method

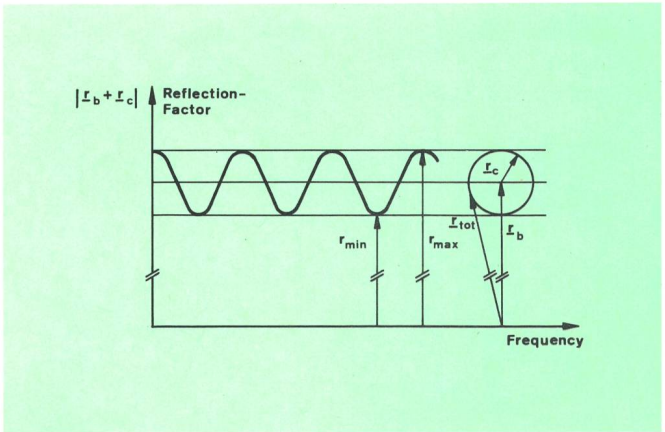

Fig. 7
Summation of reflection phasors according to set-up of Figure 6

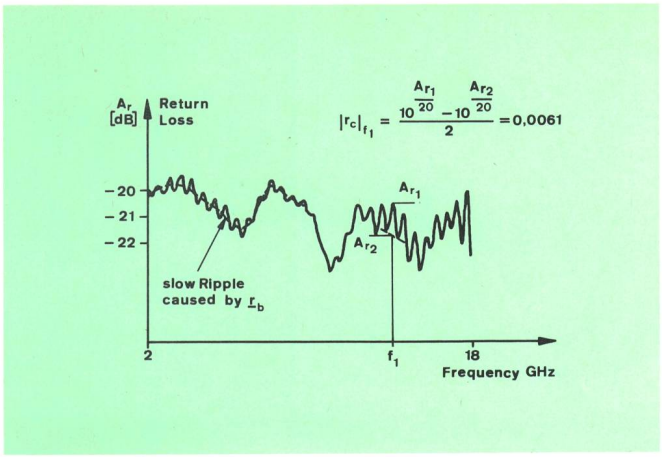

Fig. 8
Return loss measurement, example according to set-up of Figure 6

Then, the so-called offset termination with $r_A \cong 0.1$ (20 dB return Loss) is connected. By doing so, a bridge directivity of an approximate to that value is established.

The measurement method leads to a diagram of the total (resulting) reflection factor as a function of frequency, illustrated in *Figure 7.*

The summation of the two phasors representing the reflection factors as they appear at point B is shown:

$$\underline{r}_{tot} = \underline{r}_b + \underline{r}_c \qquad \text{where}$$

$\underline{r}_b$ is due to the intentional and known mismatch of the bridge at the port B and is more or less constant in amplitude. Slight deviations are caused by internal bridge errors and by the influence of non-zero line-lengths between the bridge elements and the test, respectively the reference ports.

$\underline{r}_c$ includes the reflection factor $\underline{r}_x$ of the unknown and that of the air line test connector. By its rotation relative to the phasor $\underline{r}_b$ it causes the ripple as shown in *Figure 8.*

Modern instruments use logarithmic detectors, the displayed curve will therefore show the resulting return loss in dB as ordinate and the frequency as abscissa. The conversion into reflection factor of r_c is best done by calculation, for which *Figure 8* is given as a guidance.

If the unknown device under test has to be adjusted for a given reflection factor, this can simply be done by observing the amplitude of the ripple produced by $\underline{r}_c$.

The offset reflection factor r_b must always be greater than $\underline{r}_c$ to prevent ambiguity of the total reflection.

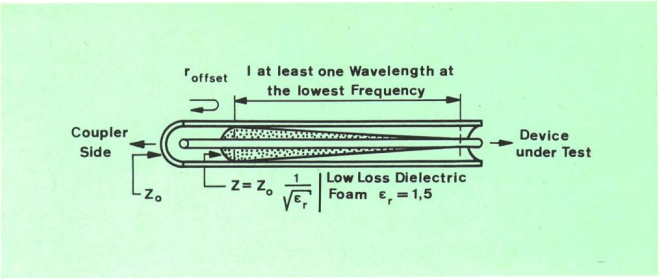

Fig. 9
Impedance step line reflection (with $\varepsilon_r = 1.5$) $r_{offset} \sim 20$ dB return loss

The swept frequency range and the electrical length of the air line should be chosen such that there is a sufficient number of ripples to determine the reflection factor curve. With a 300 mm air line l_1 between bridge test port at B and the unknown at C, one r_c-ripple period corresponds to a 500 MHz variation in the frequency axis of the display.

Sharp resonance reflections in the frequency band of interest can easily be detected. Such reflections create sharp irregularities in the reflection sum curve.

When using a directional coupler instead of a bridge, the line l_1 (from B to C) shall be replaced by an essentially frequency independent line reflection in the form of a coaxial line partially filled with dielectric foam as shown in *Figure 9,* with a sharp discontinuity at B.

The measuring process is similar to that described above for the bridge method with error recognition.

24 Measurement of two Ports with the Magnified Offset Reflection Method [3]

The measurement of small reflection factors on low loss two ports is always troublesome because of the influence of necessary adaptors and terminations. Typical examples are measurements on connectors and adaptors.

The specification of connectors poses always the problem that the reflection factor of a so-called standard connector is included in the measured reflection value of the item under test. Another approach is to measure a mated pair of connectors and the resulting reflection factor is then divided by two. Therefore, we suggest to specify connectors as mated pairs only, both mounted on suitable cables or air lines.

By adding a second air line or cable between the unknown and the termination, the reflection factor $\underline{r}_c$ of the

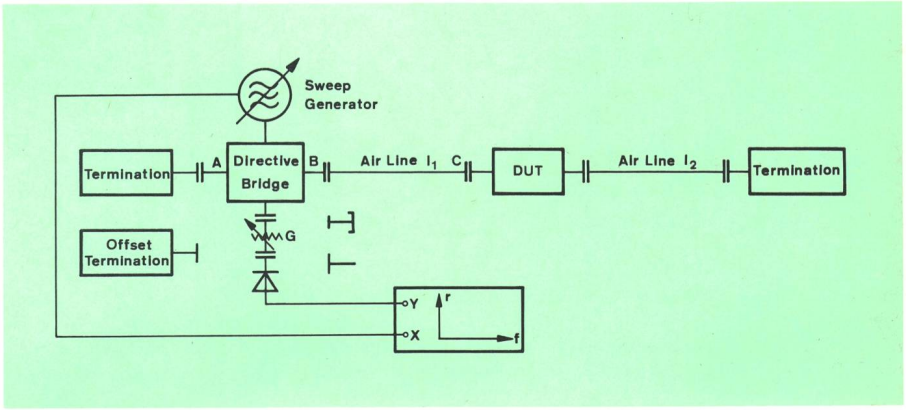

Fig. 10
Magnified offset reflection set-up with two lines

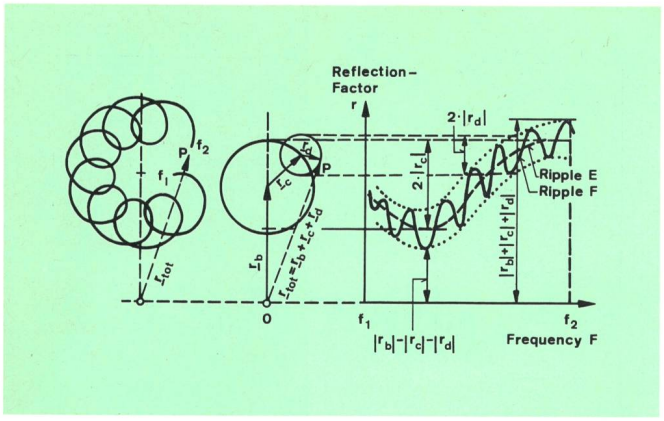

Fig. 11
Complexor (phasor) diagram, according to set-up of Figure 10

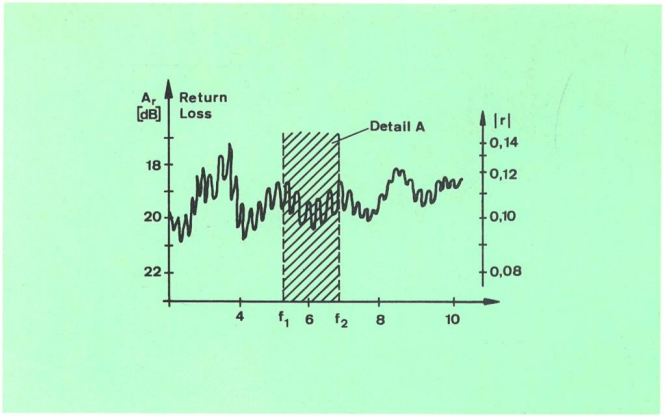

Fig. 12
Return loss measurement, example according to set-up of Figure 10

unknown can be isolated from $\underline{r}_b$ and $\underline{r}_d$ as shown in *Figure 10.*

The resulting phasor diagram shows in *Figure 11* and the suggested extraction of $\underline{r}_c$ is displayed on *Figures 12, 13* and *14.*

Alternative set-up for special purposes:

If the connector at the end of line l_1 at C or an adaptor is the test specimen to be measured, line l_2 can be replaced by an air line sliding termination. Periodic variation of the load element position (at least by one half wavelength) during the slow r.f. sweep action simulates the long line effect of a line l_2 and results in an equivalent ripple F as in Figure 11.

Remarks on remaining errors:

There are a few remaining errors not eliminated by the procedures described.

- Error caused by deviations of characteristic impedance of coaxial lines. It can be minimized by selecting the correct impedances using time domain reflectometry.
- Error of calibration attenuator G.
- Standard test connector error. It may be minimized by making the standard test connector a part of a precision air line having the same diameter.
- Influence of air line l_1 attenuation between B and C on the reflection factor value r_c measured. If this attenuation is not negligible, twice its value (in dB) has to be subtracted from the return loss before computing the true reflection factor r_c.
- Restriction to devices having smooth changing reflection characteristics.

For quick investigation of the complex phasor diagrams, simple routines for programmable pocket calculaters can be written. On *Figure 15* the program is explained.

25 Automatic Magnified Offset Reflection Factor Measurement

A small computer is added to the test set-up on Figure 10. The frequency range of interest is digitally swept and the amplitude frequency response is stored.

The unknown reflection factor is included in the composite characteristic ripple amplitude. Applying a window function to the frequency scan data allows to extract the desired ripple amplitude. With this method, the average value and data irregularities are completely eliminated. Care must be taken not to suppress real reflection factor spikes (moding, etc.) in the investigated frequency range. For that, observation of raw data is recommended.

Although the method seems very attractive, little is known on how test data are processed with steep variations in reflection factor with respect to frequency. Also, the length of the used air line implies the minimal frequency resolution.

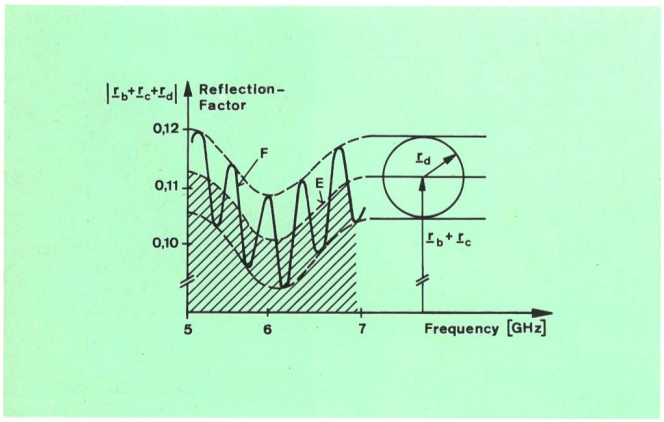

Fig. 13
Detail A, converted to reflection factor. Elimination of r_d by averaging out F. Ordinate values of shaded area corresponds to the sum $|\underline{r}_b + \underline{r}_c|$

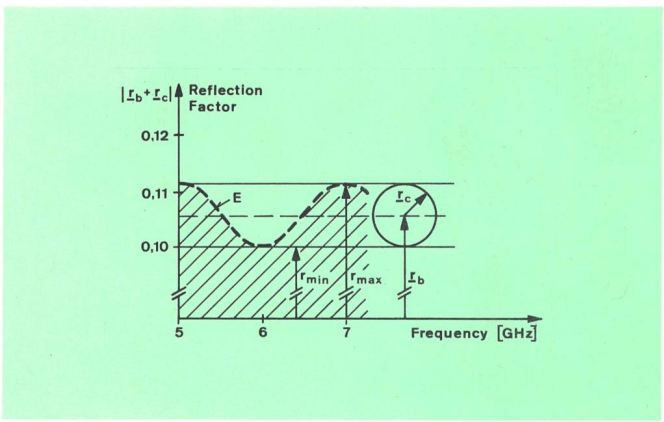

Fig. 14
Extraction of $\underline{r}_c$ (ripple E) by dividing the difference $r_{max} - r_{min}$ by two. $\underline{r}_c$ is the reflection factor of the connector under test (including the reflection of the standard connector at C of Fig. 10)

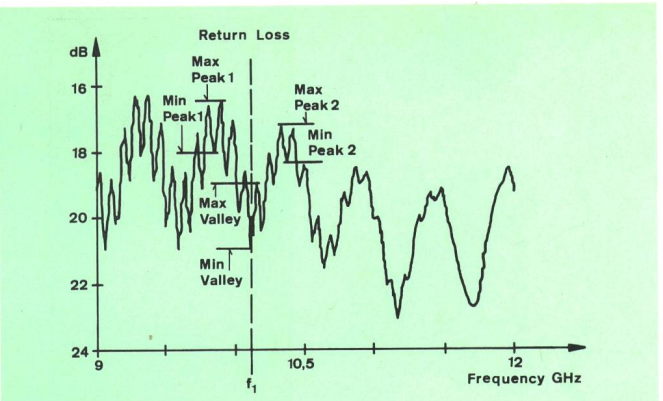


```
PROGRAM                                    EXTRACTION
FOR HP 41C                                 OF Rc

                                                          XEQ "OFFSET"
01*LBL "OFFSET"      30 PSE          59 RCL 05      EXTRACTION
02 "EXTRACTION"      31*LBL 02       60 ST+ 06      OF UNKNOWN
03 AVIEW             32 CLRG         61 2           REFLECTION
04 PSE               33 "MAX PEAK1?" 62 ST/ 06      FACTOR
05 "OF UNKNOWN"      34 PROMPT       63 RCL 02      FOR OFFSET
06 AVIEW             35 XEQ 01       64 ST+ 06      METHOD WITH
07 PSE               36 "MIN PEAK1"  65 2           2 LINES
08 "REFLECTION"      37 PROMPT       66 ST/ 06      INPUT IN
09 AVIEW             38 XEQ 01       67 RCL 04      dB VALUES
10 PSE               39 "MAX VALLEY?" 68 ST- 06     MAX PEAK1?
11 "FACTOR"          40 PROMPT       69 50                16.400000  RUN
12 AVIEW             41 XEQ 01       70 ST* 06      MIN PEAK1
13 PSE               42 "MIN VALLEY?" 71 RCL 06           18.000000  RUN
14 "FOR OFFSET"      43 PROMPT       72 "R IN %="   MAX VALLEY?
15 AVIEW             44 XEQ 01       73 ARCL X            18.800000  RUN
16 PSE               45 "MAX PEAK2 ?" 74 AVIEW      MIN VALLEY?
17 "METHOD WITH"     46 PROMPT       75 STOP              20.300000  RUN
18 AVIEW             47 XEQ 01       76 GTO 02      MAX PEAK2 ?
19 PSE               48 "MIN PEAK2 ?" 77*LBL 01           17.100000  RUN
20 "2 LINES"         49 PROMPT       78 1           MIN PEAK2.?
21 AVIEW             50 XEQ 01       79 ST+ 10            18.300000  RUN
22 PSE               51 RCL 01       80 RDN         R IN %=1.580890
23 PSE               52 ST+ 02       81 -.05
24 "INPUT IN"        53 2            82 *
25 AVIEW             54 ST/ 02       83 10†X
26 PSE               55 RCL 03       84 STO IND 10
27 "dB VALUES"       56 ST+ 04       85 RTN
28 AVIEW             57 2            86 .END.
29 PSE               58 ST/ 04
```

Fig. 15
Extraction of $\underline{r}_c$ at f_1 with programmable pocket calculator

In contrast, calibration demands only one reference which is commonly established by a short circuit. The advantage of this method is that the low reflection factor measurement is not affected by connector repeatability between a reference termination and an unknown as it is in the case of automatic network analyzer system.

Electrically short two ports (e.g. mated connectors, adaptors, etc.) can be measured by adding a second air line with termination at the output of the two ports. The window function allows to extract the ripple produced by the two-port embedded between the two reference lines. Actually, very little is known about the performance of this method.

3 Time Domain Reflectometer (TDR)

Time domain reflectometry is today a well known measuring technique, therefore a detailed description is not necessary.

The main advantage of this method is the simultaneous display of magnitude and location of the reflection factor in the tested system. Difficulties arise when interpreting displayed reflection factors in the frequency domain.

With fast rise time (system rise time ~ 35 ps) TDR, reflection factors of t $\leqq$0.01 with resolution of a few centimeters can be detected. Direct conversion to frequency domain is valid to about 3 GHz.

31 Automated Time Domain Reflectometry (ATDR) *(Fig. 16)*

The combination of a TDR and a computer allows to obtain frequency domain data with the aid of a Fast Fourier Transform Algorithm (FFT). Since TDR can resolve different distances, windowing function can be applied to refer unknown test item to a simple precision air line only. Calibration data of a short circuit must be taken previously.

Because there is no need for a directive device with limited bandwidth, an extreme broadband data is obtained with a simple test set-up. The principle application is therefore in material research (time domain spectroscopy) and in connector development. With further expense, performance similar to the best ANA can be reached [4].

A simple test set-up and an extreme broad bandwidth response (DC to 18 GHz) are advantageous. Unwanted errors during measurement are easily recognized in the time domain display (real time).

The main problem is the stabilization of the time zero point for the FFT during calibration and measurement. Also, the video feed through of the tunnel diode trigger signal may disturb the measurements. Tuning of the frequency domain response of a test item is very difficult because of slow speed of data processing. Resonance peaks can fall out in time domain and frequency domain because the FFT produces discrete frequency points depending on the data window applied to the time domain data. Residual reflections in the test system usually degrade performance beyond 6...10 GHz.

Unfortunately, the fastest TDR-Sampler System (20 ps step generator) from Hewlett-Packard is no longer available. Tektronix Inc. is still supplying its 25 ps step generator TDR.

References

[1] *Hackborn R. A.* An Automatic Network Analyzer System. Dedham, Mass., Microwave Journal 11 (1968) 5, p. 45.

[2] Mountain View, Cal., Wiltron Technical Review (1978) 8.

[3] Reflection Factor of Radio Frequency Connectors, General Requirements and Measuring Methods. Geneva, International Electrotechnical Commission, Revision of Sub-Clause 14,1 of IEC Publication 169-1, Doc 46 D (CO) 78.

[4] *Gans W. L.* and *Andrews J. R.* Time Domain Automatic Network Analyzer for Measurement of RF and Microwave Components. Washington, NBS Tech. Note 672, September 1975.

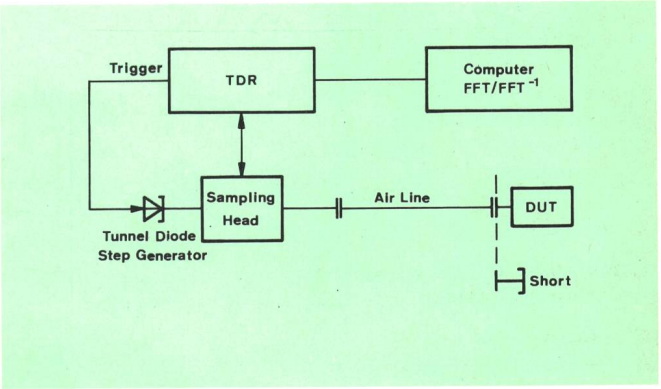

Fig. 16
Automated time domain reflectometer